



## SUCCESSFUL INSTALLATION OF ARC MELTER AT PINSTECH FOR THE SYNTHESIS OF BULK AMORPHOUS MATERIALS

\*M. IQBAL and B. AHMAD

Microstructural Studies Group, Physics Division, Directorate of Science, PINSTECH, P.O. Nilore, Islamabad, Pakistan

(Received October 20, 2010 and accepted in revised form December 06, 2010)

In this paper the results on production of  $[Zr_{0.65}Cu_{0.18}Ni_{0.09}Al_{0.08}]_{98}Nb_2$  bulk amorphous alloy synthesized by the Arc Melter WK-II are presented. The machine is installed at MSG-PD-PINSTECH for the synthesis of bulk metallic glasses (BMGs). Actually this machine is the combination of arc and induction melting furnaces with Cu mold casting facility. With the installation of this machine, it is possible to produce various types of materials locally such as bulk amorphous materials and polycrystalline materials. Both rods and sheets can be produced. The specifications of machine and procedures of materials synthesis are described. Thermal properties, crystallization behaviour and activation energy of  $[Zr_{0.65}Cu_{0.18}Ni_{0.09}Al_{0.08}]_{98}Nb_2$  BMG have been reported. Characterization of materials was done by X-ray diffraction (XRD), scanning electron microscopy (SEM) and energy dispersive spectroscopy (EDS) techniques. The alloy shows wide supercooled liquid region of more than 120 K. DSC results show double stage crystallization. The activation energy for first and second stage crystallization was calculated to be 198.6 and 156.7 kJ/mol. The  $NiZr_2$  (metastable phase) and  $CuZr_2$  (stable phase) were found in the annealed samples. XRD, DSC and EDS results are in good agreement.

**Keywords:** Amorphous alloys, Thermal properties, Crystallization, Scanning electron microscopy (SEM), Differential scanning calorimetry (DSC), Energy dispersive spectroscopy (EDS)

### 1. Introduction

Metallic materials with amorphous structure are known as bulk metallic glasses (BMGs) or bulk amorphous materials. In contrast to crystalline materials, BMGs are free from defects such as grain boundaries, dislocations and precipitates etc. They exhibit short-range atomic order and have non-equilibrium structure. BMGs have random atomic arrangement and are obtained by rapid quenching of metallic melts. Metallic materials with amorphous structure having at least 1 mm thickness are classified as BMGs. The first amorphous structure was detected in  $Au_{75}Si_{25}$  melt spun ribbon prepared by Klement et al. [1] at Caltech, USA, in 1960 by rapid quenching of the melt from 1300 °C to room temperature. BMGs have excellent physical and mechanical properties than their crystalline counterparts such as high strength, high hardness, fracture toughness, impact fracture energy, fatigue strength, elastic energy, corrosion resistance, wear resistance, viscous flow ability and good reflection ratio [2]. Comparison shows that among BMGs, Zr-based

amorphous alloys have excellent properties. The elastic limit of glassy alloys is comparable with polymers but their fracture strength is higher than Ti alloys and steels [3]. Due to very attractive properties, BMGs have numerous applications such as, optical precession materials, die materials, tool materials, cutting materials, electrode materials, corrosion resistance materials, hydrogen storage materials, ornamental materials, composite materials, writing appliance materials, sporting goods materials, metallic glassy foams and amorphous plastics. Other applications includes structural applications, electronics parts, marine and medical applications, writing instruments, solders, brazing elements, fishing/hunting bows, guns, scuba gear, micro-gears, welding elements and brazing elements [1,4]. There are many techniques used for the synthesis and processing of amorphous materials such as Cu mold casting, suction casting, die casting, flux melting and spark plasma sintering process, squeeze casting, water quenching, blow molding of BMGs, laser-induced combustion synthesis, mechanical alloying by high energy ball milling, sol

\* Corresponding author : miqbalchishti@yahoo.com

gel method and water atomization [5]. There are several criteria for alloy design such as Inoue's rules [2], Greer's confusion principle [6], criteria of valence electron atom ratio (e/a ratio) and average atomic size  $R_a$  (~0.1496 nm) in the Zr-Al-Ni-Cu systems [7, 8]. The limitation of BMGs is their low plasticity which is major hindrance in industrial applications. Efforts are going on to improve the ductility of BMGs by minor alloying method [9-11], selecting the appropriate compositions and proper elemental addition of selected elements of low (< 0.12 nm) and high (> 0.16 nm) atomic sizes. An important alloy used for certain applications is  $Zr_{41}Ti_{14}Cu_{12.5}Ni_{10}Be_{22.5}$  (known as Vitreloy) which is highly biocompatible, non-allergenic and ideal for corrosion resistant. In this paper, the results on synthesis of  $[Zr_{0.65}Cu_{0.18}Ni_{0.09}Al_{0.08}]_{98}Nb_2$  BMG produced by Arc Melter WK-II are presented. Niobium addition is beneficial for enhancement of glass-forming ability (GFA) and ductility in Zr-based alloys. SEM, EDS and XRD techniques are used for materials characterization.

## 2. Experimental

### 2.1 Materials Production by Arc Melter

In order to prepare the required amorphous  $[Zr_{0.65}Cu_{0.18}Ni_{0.09}Al_{0.08}]_{98}Nb_2$  alloy, 2-4N pure metals Zr, Ni, Cu, Al and Nb were cut, precisely weighted, washed and ultrasonically cleaned in ethanol before melting in Arc Melter (WK-II) which is shown in Figure 1(a). This is the first machine in Pakistan installed at Microstructural Studies Group (MSG), Physics Division (PD), PINSTECH for the production of BMGs. The metals were melted under Ar atmosphere and Ti was used as an oxygen getter during the melting. Melting of the mixture of the required materials was done at least four times to get the extended chemical homogeneity and to achieve uniform composition of the alloy by changing sides of alloy buttons. Ingots of 5 mm diameter and 70 mm length were synthesized using Arc Melter comprising of Cu mold casting technique by applying suction casting method. The inner portion of Arc Melter consisted of Cu hearth, melting cavities, tungsten arc finger and handling spoon are shown in Figure 1(b) while Figure 1(c, d) shows the outer and inner view of Cu molds used for casting. The vacuum used for alloy casting was as low as  $1 \times 10^{-4}$  Pa. High purity (5N pure) Ar was flushed before melting and casting. For structural analysis, X-ray diffraction (XRD) was carried out using  $CuK_{\alpha 1}$  radiation ( $\lambda = 1.54056 \text{ \AA}$ ). The samples taken from the centers of ingots were

cut and fine polished on lapping machine for characterizations and were examined in scanning electron microscope (SEM) and microanalysis was carried out by EDS (energy dispersive spectroscopy) attached with SEM. In order to evaluate the thermal parameters, differential scanning calorimetry (DSC) was performed using NETZSCH DSC 404C at different heating rates under Ar atmosphere. Activation energy was calculated by Kissinger method.

### 2.2 Major Parts and Operational Parameters of Arc Melter

In the Arc Melter WK-II, there are four melting cavities and about 70 g material can be melted in each cavity. The fifth central cavity is used for casting using Cu molds. At a time 4 samples of same type can be melted one by one in a single run. Presently in Arc Melter WK-II, ingots of 3, 5 and 10 mm diameters and 70 mm length and sheets of 1mm thickness and 70 mm length can be cast. Length of ingots is adjustable. Most of the metallic elements can be melted but avoid melting of Mg, toxic and radioactive elements. Be careful during melting and casting, follow all precautionary measures and use goggles. The Arc Melter WK-II consists of furnace chamber of cylindrical shape having diameters of 306 mm x 340 mm and made of stainless steel stove body, Cu hearths, tungsten arc finger, Cu molds casters, control unit and an electric welding machine. The major systems involved are vacuum system, electrical system and water cooling auto alarm system. The working medium is high purity Ar gas and Ti getter but mixing method is manual.

## 3. Results and Discussion

### 3.1 Characterization of Material by XRD, SEM and EDS

Physical examination of the alloy ingots show highly metallic luster. It indicates amorphous structure. Figure 2 shows XRD patterns of the as cast sample of 5 mm diameter taken from the center of the alloy ingots. The broad bands observed in 2 theta range of 30-45 degrees show amorphous structure of the alloy studied. The alloy show high glass-forming ability (GFA). SEM examination shows featureless surface. It confirms the amorphous nature of the alloy. The EDS analysis was done in many areas which show almost uniform alloy composition. Figure 2 shows

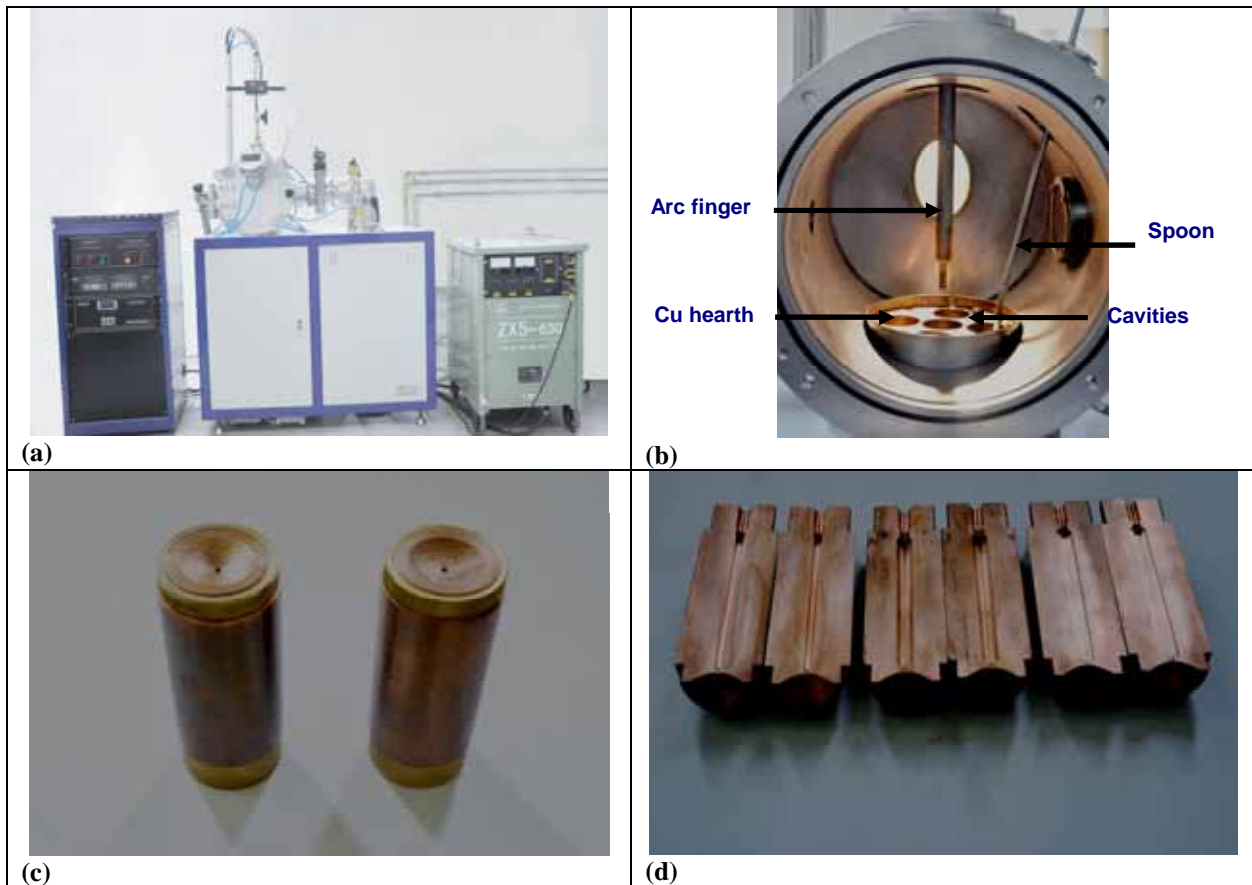


Figure 1. (a) Arc melter installed at PINSTECH (b) inner view of the chamber (c) copper molds and (d) inner view of molds.

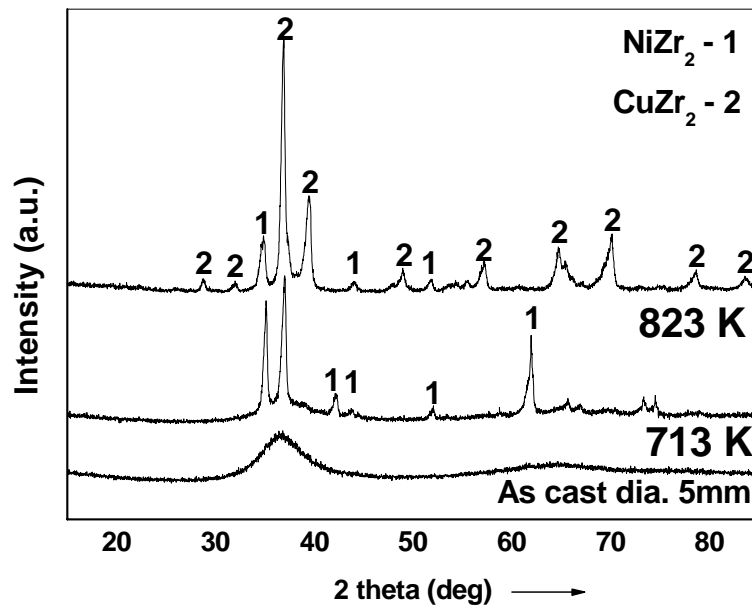


Figure 2. XRD pattern of the as cast and samples annealed at different temperatures.

XRD patterns of the samples annealed at 713 and 823 K for 20 minutes each. Two phases, NiZr<sub>2</sub> (metastable) and CuZr<sub>2</sub> are identified in the annealed samples. The results show that initially primary phase NiZr<sub>2</sub> (known as Laves phase), nucleated at annealing temperature 713 K. The CuZr<sub>2</sub> stable phase nucleated later at 823 K. The reason is higher negative heat of mixing ( $\Delta H_{mix}$ ) of Ni-Zr pair (-49 kJ/mol) than Cu-Zr pair (-23 kJ/mol) [12]. Another reason is that Ni has the smallest atomic size (0.12459 nm) than all alloy constituents [13] and can easily interact with solvent Zr. With rise in temperature, intensity of NiZr<sub>2</sub> phase decreases while peaks of CuZr<sub>2</sub> phase become stronger. The XRD results show that amount of NiZr<sub>2</sub> phase is maximum at 713 K while it reduces at 823 K. The amount of crystallization is maximum at 823 K. Niobium does not interact with Zr or any other element. The reason is positive heat of mixing of Zr-Nb and Cu-Nb pairs and larger atomic size of Nb than Ni and Cu. Mixing enthalpies and atomic radii of all the alloy constituents are given in Table 1.

### 3.2 Characterization by Differential Scanning Calorimetry (DSC)

Figure 3 (a-c) shows high and low temperature DSC at different heating rates. Glass transition temperature  $T_g$ , crystallization temperature  $T_x$ , peak temperature  $T_p$ , melting temperature  $T_m$  and liquidus temperature  $T_l$  were determined. From the basic thermal parameters, width of supercooled liquid region  $\Delta T_x = T_x - T_g$ , a key parameter known as reduced glass transition temperature  $T_{rg1} = T_g/T_m$  and  $T_{rg2} = T_g/T_l$  and other thermal parameters like  $\gamma = T_x/(T_l + T_g)$  [14],  $\delta = T_x/(T_l - T_g)$  [15],  $\beta = T_g \cdot T_x / (T_l - T_x)^2$  [16] and a newly defined thermal parameter  $\omega = T_g/T_x - 2T_g/(T_g + T_l)$  [17] were calculated and results are summarized in Table 2(a, b) for the alloy studied. These parameters are also GFA indicators and indicate clear thermal behavior of the materials. These parameters are actually relative ratios of basic thermal parameters. In addition, Weinberg parameter  $K_W = (T_x - T_g)/T_m$ , Hruby parameter [18]  $K_H = (T_x - T_g)/(T_m - T_x)$ , thermal parameter  $K_{LL} = T_x/(T_g + T_m)$  proposed by Lu and Liu,  $K_1 = T_m - T_g$ ,  $K_2 = \Delta T_x$ ,  $K_3 = T_x/T_m$ ,  $K_4 = (T_p - T_x)/(T_x -$

Table 1. Mixing enthalpies and atomic radii of alloy constituents.

Alloy elements	Atomic radii (nm)	Mixing enthalpies (kJmol <sup>-1</sup> )			
		Zr	Al	Ni	Cu
		0.16025	0.14317	0.12459	0.12780
Zr	0.16025	-	-44	-49	-23
Al	0.14317	-44	-	-22	-1
Nb	0.14290	4	-18	-30	3
Cu	0.12780	-23	-1	4	-
Ni	0.12459	-49	-22	-	4

Table 2a. Thermal parameters of the alloy studied at heating rate "r". (All temperatures are in K).

r	$T_g$	$T_x$	$\Delta T_x$	$T_m$	$T_l$	$T_{rg1}$	$T_{rg2}$	$\gamma$	$\delta$	$\beta$	$\omega$
10	584	708	124	1102	1142	0.530	0.511	0.410	1.269	2.20	0.148
20	616	737	121	1100	1116	0.560	0.552	0.425	1.473	3.16	0.125

Table 2b. A few more thermal parameters of the alloy derived from DSC results.

r	$T_p$	$K_W$	$K_{LL}$	$K_H$	$K_{SP}$	$K_1$	$K_2$	$K_3$	$K_4$
10	712.5	0.113	0.420	0.315	0.956	518.0	124	0.642	0.509
20	753.0	0.110	0.429	0.333	3.143	484.2	121	0.670	1.76

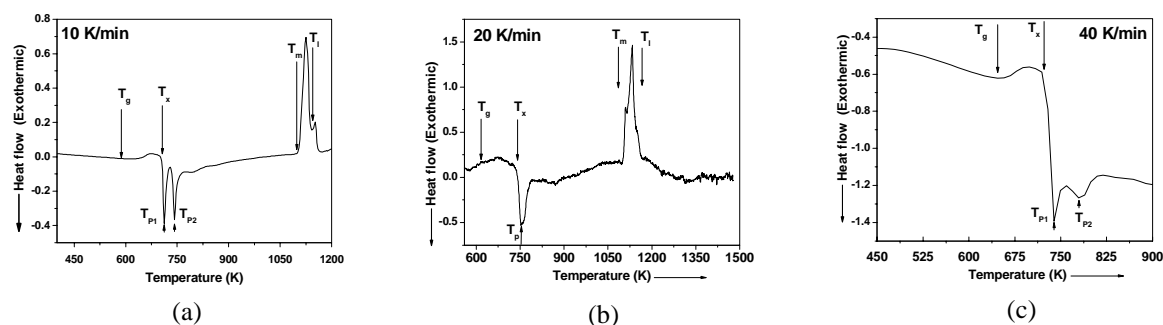


Figure 3 (a-c). (a) High temperature DSC of the alloy at 10 K/min, (b) 20 K/min (b) and (c) low temperature DSC at 40 K/min.

$T_g/T_m$  and stability parameter  $K_{SP} = (T_p - T_x)(T_x - T_g)/T_g$  suggested by Saad and Poulain [19-21] are also calculated for all the alloys. The results indicate that the alloy studied has very wide supercooled liquid region of more than 120 K. Reduced glass transition temperatures  $T_{rg}$ ,  $\gamma$  and  $\beta$  parameters are very promising. The significant difference in  $K_{SP}$  at heating rate of 20 K/min is due to high difference between  $T_p$  and  $T_x$ . XRD and DSC results confirm each other. Double stage crystallization was observed in the alloy.

### 3.3 Calculation of the Activation Energy by Kissinger Plots

The activation energy required for crystallization of an alloy is an important kinetic parameter for the determination of thermal stability of amorphous phase. Based on the results of the exothermic peak shifting in DSC measurements conducted at different heating rates, the value of activation energy was calculated by Kissinger equation [22]. The dependency of crystallization temperature on heating rate was used to determine the associated activation energy “ $E_{ac}$ ” by means of Kissinger’s equation  $\ln(r/T_p^2) = -E_{ac}/RT_p + \text{constant}$  where “ $r$ ” is the heating rate,  $T_p$  is the peak temperature in DSC scans,  $R$  is the gas constant  $\sim 8.3145$  J/mol-K, with slope  $B = -E_{ac}/R$ , where  $B$  is a constant. Figure 4 shows two Kissinger plots for calculations of activation energies for 1<sup>st</sup> and 2<sup>nd</sup> stage crystallizations  $E_{ac1}$  and  $E_{ac2}$  using peak temperatures  $T_{p1}$  and  $T_{p2}$  respectively. The plot of  $\ln(r/T_p^2)$  plots versus  $1000/T_p$  ( $K^{-1}$ ) was plotted for determination of slope  $B$  to calculate activation energies. The designations  $E_{ac1}$  and  $E_{ac2}$  stand for 1<sup>st</sup> and 2<sup>nd</sup> stage activation energy. The activation energy for first and second stage crystallization was calculated to be 198.6 and 156.7 kJ/mol. It shows good thermal stability of the alloy against crystallization.

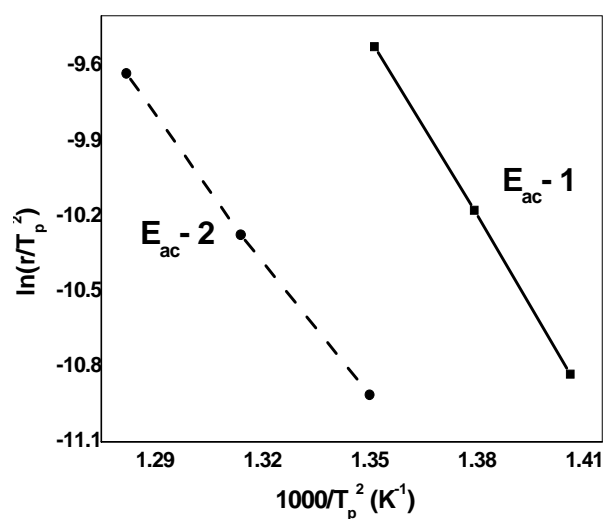


Figure 4. Kissinger plots of the alloy.  $E_{ac-1}$  and  $E_{ac-2}$  show activation energy of first and second stage crystallization.

## 4. Conclusions

With the installation of Arc Melter WK-II at PINSTECH, it is possible to produce amorphous materials in Pakistan. Bulk amorphous ingots of 5 mm diameter of  $[Zr_{0.65}Cu_{0.18}Ni_{0.09}Al_{0.08}]_{98}Nb_2$  alloy were produced. The alloy show wide supercooled liquid region of more than 120 K and high glass-forming ability. Double stage crystallization was observed. The metastable phase  $NiZr_2$  and stable phase  $CuZr_2$  were identified in the annealed samples by XRD and confirmed by EDS. Examination in SEM shows featureless surface which confirm amorphous structure. The EDS analysis shows uniform composition. XRD, DSC and EDS results are in good agreement.

## Acknowledgements

The authors gratefully acknowledge the financial support provided by PAEC for Arc Melter. Thanks to Dr. J.I. Akhter, Dr. Javed Bashir and Dr. Maqsood Ahmad for their cooperation. The major contribution of Mr. Naeem Akhtar PD, PINSTECH in the installation of Arc Melter is highly appreciated. Technical help provided by all officials of MSG-PD, GSD and ED officials especially Mr. Khalil Subhan, Idrees Khattak, Mr. Khalid (ED) and CDL officials are acknowledged. Thanks to Mr. Basit (GSD) for significant contribution. The technical support by Prof. W.H. Wang, IOP, Beijing, China is highly appreciated.

## 5. References

- [1] W. Klement, R.H. Willens and P. Duwez, *Nature* **187** (1960) 869.
- [2] A. Inoue, *Acta Mater.* **48** (2000) 279.
- [3] M. Telford, *Mater. Today.* **7** (2004) 36.
- [4] M. Iqbal and J.I. Akhter, *Key Eng. Mater.* **442** (2010) 41.
- [5] M. Iqbal, Ph. D. Dissertation, Institute of Metal Research, Chinese Academy of Sciences, Shenyang, China, May (2008).
- [6] A.L. Greer, *Nature* **366** (1993) 303.
- [7] W. Chen, Y. Wang, J. Qiang and C. Dong, *Acta Mater.* **51** (2003) 1899.
- [8] C. Dong, Y.M. Wang, J.B. Qiang, D.H. Wang, W.R. Chen and C.H. Shek, *Mater. Trans.* **45** (2004) 1177.
- [9] W. H. Wang, *Prog. Mater. Sci.* **52** (2007) 540.
- [10] M. Iqbal, W.S. Sun, H.F. Zhang, J.I. Akhter and Z.Q. Hu, *Mater. Sci. Eng. A* **447** (2007) 167.
- [11] Z.P. Lu and C.T. Liu, *J. Mater. Sci.* **39** (2004) 3965.
- [12] A. Takeuchi and A. Inoue, *Mater. Trans.* **46** (2005) 2817.
- [13] O.N. Senkov and D.B. Miracle, *Mater. Res. Bull.* **36** (2001) 2183.
- [14] Z.P. Lu, H. Bei and C.T. Liu, *Intermetallics* **15** (2007) 618.
- [15] Q.J. Chen, J. Shen, D.L. Zhang, H.B. Fan, J. F. Sun and D.G. McCartney, *Mater. Sci. Eng. A* **433** (2006) 155.
- [16] Z.Z. Yuan, S.L. Bao, Y. Lu, D. P. Zhang and L. Yao, *J. Alloy. Compd.* **459** (2008) 251.
- [17] Z.L. Long, G. Xie, H. Wei, J. Peng, P. Zhang and A. Inoue, *Mater. Sci. Eng. A* **509** (2009) 23.
- [18] A. Hruby, *Czech. J. Phys.* **B 22** (1972) 1187.
- [19] M. Saad and M. Poulain, *Mater. Sci. Forum* **19** (1987) 11.
- [20] M.L.F. Nascimento, L.A. Souza, E.B. Ferreira and E.D. Zanotto, *J. Non-Cryst. Solids* **351** (2005) 3296.
- [21] Y. Li, *J. Mater. Sci. Technol.* **15** (1999) 97.
- [22] H.E. Kissinger, *Ana. Chem.* **29** (1957) 1702.